Journal of Organometallic Chemistry, 290 (1985) 353–364
Elsevier Sequoia S.A., Lausanne – Printed in The Netherlands

OPTICALLY ACTIVE TRANSITION METAL COMPOUNDS

LXXXI*. CRYSTAL STRUCTURE OF $(+)_{546}$-$[C_5H_5Mo(CO)_2LL^*]PF_6$ (LL^* = 2-BENZOYLPYRIDINE-(*R*)-1-PHENYLETHYLIMINE)

IVAN BERNAL, WOLFGANG RIES,

Department of Chemistry, University of Houston, Houston, Texas (U.S.A.)

HENRI BRUNNER, and DEVENDRA K. RASTOGI

Institut für Anorganische Chemie, Universität Regensburg, Universitätsstr. 31, Regensburg (West Germany)

(Received February 7th, 1985)

Summary

Racemic $[C_5H_5Mo(CO)_2LL^*]PF_6$ (**2**) with LL^* = 2-benzoylpyridine-1-phenylethylimine, undergoes spontaneous resolution upon crystallization from acetone/CH_2Cl_2/ethanol. The absolute configuration of the $(+)_{546}$-isomer was shown to be (*R*) at the Mo atom and (*R*) at the asymmetric carbon atom. Comparison of **2** with $[C_5H_5Mo(CO)_2LL^*]PF_6$ (**1**) (LL^* = 2-carbaldehydepyridine-1-phenylethylimine) reveals distinct changes caused by the differences resulting from the presence of the phenyl group in **2** and the change from the (*RR*)- to the (*RS*)-configuration.

Introduction

The complex $[C_5H_5Mo(CO)_2LL^*]PF_6$ (**1**), where LL^* is the Schiff base from pyridine-2-carbaldehyde and (*S*)-1-phenylethylamine, has been described as having a "four-legged-piano-stool" square-pyramidal geometry [2]. It forms a pair of diastereoisomers which differ only in the configurations, *R* or *S*, at the asymmetric Mo atom. The diastereoisomers *RS* and *SS* can be separated; they equilibrate to an *RS*/*SS* 30/70 ratio with a half life of 30 min at 70°C in acetone solution [3]. The absolute configuration of the thermodynamically less stable isomer *RS* was determined by X-ray diffraction [4,5].

Conformational analyses on a series of $C_5H_5Mo(CO)_2LL^*$ compounds in which LL^* was a thioamidato or amidinato anion, showed that of the various conforma-

* For part LXXX see ref. 1.

0022-328X/85/$03.30

tions which the (*S*)-1-phenylethyl group at the nitrogen atom can adopt by rotation about the single C–N bond, the molecule prefers specific arrangements determined by intramolecular attractions and repulsions [6–8]. These conformational studies were extended from 4-membered to 5-membered chelate rings [9,10], and the substituent at the imine carbon atom turned out to have a critical influence on the $R^* = CH(Me)(Ph)$ conformation and the thermodynamic stability of a given diastereomer. We now present the results of an X-ray structural analysis of $[C_5H_5Mo(CO)_2LL^*]PF_6$ (**2**) with LL^* = Schiff base of 2-benzoylpyridine and (*R*)-1-phenylethylamine, and make a detailed comparison of the stereochemistry of **1** and **2** which reveals the changes caused by the introduction of a phenyl group in place of hydrogen on going from **1** to **2** and the change from the (*S*)-configuration of the ligand in **1** (*RS*) to the (*R*) configuration in **2** (*RR*).

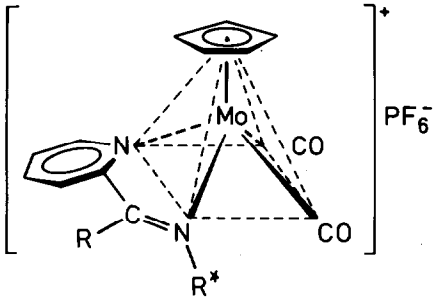

1:R = H ; R^* = (S)–CH(Me)(Ph)
2:R = Ph ; R^* = (R) CH(Me)(Ph)

Experimental

For the preparation of compound **2**, the optically active Schiff base derived from 2-benzoylpyridine and (*S*)-(−)-1-phenylethylamine was used. The ligand racemized during the reaction, as previously described [9,10]. A mixture of the two diastereoisomeric pairs of enantiomers *RR/SS* and *RS/SR* (Mo configuration given first, C configuration second) was formed in 56 : 44 ratio [10]. Fractional crystallization from 16/2/1 acetone/CH_2Cl_2/ethanol, gave the diastereomerically pure, less soluble pair of enantiomers, showing a high field C_5H_5 signal at τ 4.00 but no bulk optical activity. A crystal from this sample was used for the X-ray structure analysis.

A small purple crystal of **2** was ground to a spherical shape in an ENRAF–NONIUS spherizer and mounted on an X–Y–Z translation head. A set of 25 reflections appropriately spread over reciprocal space and having $20° \leqslant 2\theta \leqslant 40°$ was used to define orientation and Niggli matrices, the latter indicating that the lattice was primitive. Search for absences and LAUE symmetry confirmed that the space group was $P2_1$ or $P2_1/m$; since the Schiff base ligand used was racemic [10], we could not be sure at this stage which was correct. A data set was collected, details of all crystallographic parameters being summarized in Table 1. Examination of the distribution of unitary structure factors suggested the acentric space group to be correct. This was verified by the solution and refinement of the structure and by the fact that for $Z = 2$ the cation would have to be on a mirror plane in $P2_1/m$, which is impossible in the absence of molecular disorder in the lattice.

TABLE 1

SUMMARY OF DATA COLLECTION AND PROCESSING PARAMETERS FOR **2**

Space Group	$P2_1$
Cell constants	a 10.361 (4) Å
	b 15.602 (9) Å
	c 10.920 (4) Å
	β 99.27 (3)°
Cell volume	V 1742.3 Å^3
Molecular formula	$C_{27}H_{23}F_6MoN_2O_2P \cdot 2(C_3H_6O)$
Molecular weight	764.56
Density (calc; Z = 2)	ρ 1.46 g cm^{-3}
Radiation	Mo-K$_\alpha$ (λ 0.71609 Å)
Absorption coefficient	μ 4.93 cm^{-1}
Data collection range	$4° \leqslant 2\theta \leqslant 60°$
Scan width	$\Delta\theta = (1.00 + 0.35 \tan\theta)°$
Maximum scan time	240 s
Scan speed range	0.39 to 5.03 ° min^{-1}
Total data collected	5037
Data with $I > 3\sigma(I)$	2372
Total variables	295
$R = \Sigma \mid\mid F_0 \mid - \mid F_c \mid\mid / \Sigma \mid F_0 \mid$	0.058
$R_w = [\Sigma w(\mid F_0 \mid - \mid F_c \mid)^2 / \Sigma w \mid F_0 \mid^2]^{1/2}$	0.076
Weights	$w = 1.00/(\sigma^2(F) + 0.0059F^2)$
Goodness of fit	0.87

The crystal decomposed a little during the data collection because of loss of acetone of crystallization. The decay was linear and nearly identical for all three standard reflections used ($\bar{1}$ 6 3; 0 5 4; 1 5 6) and, so, the data were corrected as described elsewhere [11]; this did not improve the results and so the original set of uncorrected data was used for the final calculations. The SHELX-76 [12] system of programs was used throughout. The structure was solved by the heavy atom method followed by the usual cycles of refinement and difference Fourier syntheses. At this stage it became evident that the PF_6^- anion had a large amplitude of thermal motion, as usual. Therefore, it was refined as a rigid body using the routine DFIX [12] and a constant P–F distance of 1.573 Å. Similarly, the Cp ring was refined as a rigid body with C–C 1.420 Å, C–H 1.00 Å and individual, isotropic thermal parameters for all ten Cp atoms. The other hydrogens were assigned variable, isotropic thermal parameters, and all other atoms anisotropic parameters.

A difference Fourier synthesis at this stage revealed the presence of the two acetone molecules of crystallization and the origin of the crystal decay. The thermal parameters of all the acetone carbon and oxygen atoms were high and so they were fixed at isotropic values of 0.080 and their individual occupancies refined. A very uniform value of ca. 70% was obtained for all 6 carbons and 2 oxygens. Consequently, a fixed occupancy factor of 70% was assigned to these atoms and the positional and isotropic thermal parameters were refined to the final $R = 0.058$ and $R_w = 0.076$ (Table 2). Bond lengths and angles are given in Tables 3 and 4. Lists of thermal parameters and structure factors may be obtained from the authors.

The structure of the molecule is shown in Fig. 1 which also shows the numbering used. Figure 2 is a packing diagram and Figure 3 a double stereodrawing superim-

TABLE 2

ATOMIC COORDINATES for 2

Atom	x/a	y/b	z/c
Mo	0.84930(7)	0.69300(0)	0.80756(6)
O(1)	0.7465(17)	0.7795(8)	0.5558(10)
O(2)	0.7405(12)	0.5514(7)	0.6141(10)
N(1)	0.7684(8)	0.8089(5)	0.8778(8)
N(2)	0.7104(8)	0.6504(6)	0.9314(7)
C(1)	0.7874(14)	0.7474(9)	0.6517(11)
C(2)	0.7783(13)	0.5967(9)	0.6944(11)
C(8)	0.7967(13)	0.8870(8)	0.8428(12)
C(9)	0.7562(16)	0.9580(8)	0.8991(14)
C(10)	0.6763(15)	0.9498(8)	0.9941(14)
C(11)	0.6459(12)	0.8689(8)	1.0257(11)
C(12)	0.6907(11)	0.7956(8)	0.9687(10)
C(13)	0.6617(9)	0.7099(6)	0.9936(8)
C(14)	0.5787(8)	0.6880(10)	1.0929(8)
C(15)	0.4433(10)	0.7042(10)	1.0674(10)
C(16)	0.3731(10)	0.6864(13)	1.1654(11)
C(17)	0.4325(16)	0.6633(9)	1.2805(13)
C(18)	0.5615(14)	0.6556(8)	1.3001(11)
C(19)	0.6383(12)	0.6687(7)	1.2106(9)
C(20)	0.6718(13)	0.5609(8)	0.9515(10)
C(21)	0.7933(15)	0.5040(9)	0.9952(12)
C(22)	0.5835(11)	0.5255(6)	0.8370(10)
C(23)	0.5947(13)	0.4414(7)	0.7963(12)
C(24)	0.5037(18)	0.4118(9)	0.6987(13)
C(25)	0.4131(17)	0.4628(12)	0.6351(17)
C(26)	0.4033(17)	0.5477(12)	0.6737(18)
C(27)	0.4837(11)	0.5790(8)	0.7734(10)
P	0.0432(3)	0.5611(2)	0.3821(3)
F(1)	0.0380(3)	0.5202(2)	0.5129(3)
F(2)	0.1782(3)	0.5155(2)	0.3786(3)
F(3)	0.0485(3)	0.6019(2)	0.2514(3)
F(4)	0.1171(3)	0.6414(2)	0.4466(3)
F(5)	−0.0917(3)	0.6067(2)	0.3857(3)
F(6)	−0.0306(3)	0.4807(2)	0.3177(3)
O(3)	0.3854(18)	0.8043(11)	0.8014(13)
O(4)	1.0174(14)	0.8714(16)	0.1627(17)
C(3)	1.0474(10)	0.6666(5)	0.7530(7)
C(4)	1.0512(10)	0.7522(5)	0.7985(7)
C(5)	1.0438(10)	0.7488(5)	0.9271(7)
C(6)	1.0355(10)	0.6612(5)	0.9610(7)
C(7)	1.0378(10)	0.6104(5)	0.8534(7)
C(30)	0.4171(18)	0.7889(11)	0.5957(13)
C(31)	0.3927(18)	0.8387(11)	0.7028(13)
C(32)	0.3804(18)	0.9312(11)	0.6853(13)
C(40)	0.8909(14)	0.8490(16)	0.3195(17)
C(41)	1.1325(14)	0.8372(16)	0.3586(17)
C(42)	1.0129(14)	0.8522(16)	0.2693(17)
H(3)	1.0510(10)	0.6491(5)	0.6655(7)
H(4)	1.0578(10)	0.8055(5)	0.7488(7)
H(5)	1.0444(10)	0.7993(5)	0.9837(7)
H(6)	1.0292(10)	0.6391(5)	1.0457(7)
H(7)	1.0333(10)	0.5463(5)	0.8491(7)
H(8)	0.8531(13)	0.8913(8)	0.7769(12)

TABLE 2 (continued)

Atom	x/a	y/b	z/c
H(9)	0.7818(16)	1.0157(8)	0.8709(14)
H(10)	0.6468(15)	1.0021(8)	1.0349(14)
H(11)	0.5882(12)	0.8623(8)	1.0902(11)
H(15)	0.3999(10)	0.7304(10)	0.9878(10)
H(16)	0.2753(10)	0.6850(13)	1.1477(11)
H(17)	0.3814(16)	0.6524(9)	1.3492(13)
H(18)	0.6065(14)	0.6411(8)	1.3855(11)
H(19)	0.7359(12)	0.6652(7)	1.2295(9)
H(20)	0.6138(13)	0.5557(8)	1.0250(10)
H(21A)	0.7532(15)	0.4408(9)	1.0044(12)
H(21B)	0.8813(15)	0.4989(9)	0.9543(12)
H(21C)	0.8162(15)	0.5334(9)	1.0855(12)
H(23)	0.6636(13)	0.4030(7)	0.8418(12)
H(24)	0.5133(18)	0.3521(9)	0.6677(13)
H(25)	0.3497(17)	0.4414(12)	0.5628(17)
H(26)	0.3323(17)	0.5844(12)	0.6279(18)
H(27)	0.4717(11)	0.6393(8)	0.8012(10)

posing the cations of **1** and **2**. ORTEP [13] was used to generate Figs. 1 and 2, and BMFIT [14] to generate Fig. 3. Relevant planes are given in Table 5.

On the basis of 18 reflections, showing large Bijvoet differences [15,16] (Table 6,

TABLE 3

INTRAMOLECULAR BOND DISTANCES [a] IN **2**

Mo–N(1)	2.180(8)	C(14)–C(15)	1.408(14)
Mo–N(2)	2.228(8)	C(15)–C(16)	1.415(16)
Mo–C(1)	1.918(12)	C(16)–C(17)	1.358(20)
Mo–C(2)	2.007(13)	C(17)–C(18)	1.324(20)
Mo–C(3)	2.264(9)	C(18)–C(19)	1.371(16)
Mo–C(4)	2.301(10)	C(19)–C(14)	1.367(13)
Mo–C(5)	2.382(9)	C(20)–C(21)	1.549(19)
Mo–C(6)	2.396(9)	C(20)–C(22)	1.530(16)
Mo–C(7)	2.324(9)	C(22)–C(23)	1.393(15)
Mo–Cent [c]	1.997	C(23)–C(24)	1.384(20)
C(1)–O(1)	1.178(16)	C(24)–C(25)	1.336(24)
C(2)–O(2)	1.145(14)	C(25)–C(26)	1.396(24)
N(1)–C(8)	1.321(15)	C(26)–C(27)	1.352(18)
N(1)–C(12)	1.390(14)	C(27)–C(22)	1.420(18)
N(2)–C(13)	1.298(12)	P–F [b]	1.573
N(2)–C(20)	1.477(15)	C(31)–O(3)	1.217
C(8)–C(9)	1.363(18)	C(31)–C(30)	1.460
C(9)–C(10)	1.433(19)	C(31)–C(32)	1.454
C(10)–C(11)	1.356(18)	C(42)–O(4)	1.211
C(11)–C(12)	1.414(16)	C(42)–C(41)	1.467
C(12)–C(13)	1.404(15)	C(42)–C(40)	1.456
C(13)–C(14)	1.527(13)		

[a] The cyclopentadienyl C–C distances were kept at the idealized value of 1.420 Å with d(CH) 1.00 Å. [b] Refined for all P–F bonds in the isotropic stage and PF_6 kept as a rigid body during anisotropic refinement. [c] Cent denotes the geometrical center of the Cp ring.

TABLE 4

INTRAMOLECULAR BOND ANGLES FOR **2**

N(1)–Mo–N(2)	73.2(3)	C(15)–C(14)–C(19)	120.7(9)
N(1)–Mo–C(1)	81.6(5)	C(14)–C(15)–C(16)	115.5(1.0)
N(1)–Mo–C(2)	135.4(5)	C(15)–C(16)–C(17)	122.8(1.0)
N(1)–Mo–Cent	111.2(2)	C(16)–C(17)–C(18)	118.0(1.2)
N(2)–Mo–C(1)	121.0(5)	C(17)–C(18)–C(19)	123.8(1.2)
N(2)–Mo–C(2)	86.8(4)	C(18)–C(19)–C(14)	118.5(1.1)
N(2)–Mo–Cent	122.5(2)	N(2)–C(20)–C(21)	111.1(1.1)
C(1)–Mo–C(2)	75.3(6)	N(2)–C(20)–C(22)	111.0(8)
C(1)–Mo–Cent	116.3(5)	C(21)–C(20)–C(22)	113.3(1.0)
C(2)–Mo–Cent	113.2(4)	C(20)–C(22)–C(23)	122.0(1.1)
Mo–N(1)–C(8)	123.0(7)	C(20)–C(22)–C(27)	118.8(9)
Mo–N(1)–C(12)	115.3(7)	C(23)–C(22)–C(27)	119.1(1.1)
C(8)–N(1)–C(12)	121.7(9)	C(22)–C(23)–C(24)	118.5(1.4)
Mo–N(2)–C(13)	116.7(7)	C(23)–C(24)–C(25)	122.5(1.3)
Mo–N(2)–C(20)	126.0(7)	C(24)–C(25)–C(26)	119.0(1.5)
C(13)–N(2)–C(20)	117.3(8)	C(25)–C(26)–C(27)	121.3(1.7)
Mo–C(1)–O(1)	178.2(1.3)	C(26)–C(27)–C(22)	119.3(1.3)
Mo–C(2)–O(2)	168.3(1.1)	O(3)–C(31)–C(30)	121.2
N(1)–C(8)–C(9)	121.1(1.0)	O(3)–C(31)–C(32)	122.4
C(8)–C(9)–C(10)	120.6(1.0)	C(30)–C(31)–C(32)	116.4
C(9)–C(10)–C(11)	116.9(1.1)	O(4)–C(42)–C(41)	121.4
C(10)–C(11)–C(12)	122.1(1.1)	O(4)–C(42)–C(40)	122.7
C(11)–C(12)–N(1)	117.5(1.0)	C(40)–C(42)–C(41)	115.8
C(11)–C(12)–C(13)	125.9(1.0)		
N(1)–C(12)–C(13)	116.6(9)		
C(12)–C(13)–N(2)	117.6(8)		
C(12)–C(13)–C(14)	120.8(9)		
N(2)–C(13)–C(14)	121.6(9)		
C(13)–C(14)–C(15)	118.4(9)		
C(13)–C(14)–C(19)	119.7(8)		

the absolute configuration *RR* was assigned to the asymmetric Mo and C atoms, respectively (Fig. 1, Table 2). For the specification of the Mo configuration, **2** being a *b*-type chiroid [17–19], the priority sequence C_5H_5 > N(imine) > N(pyridine)

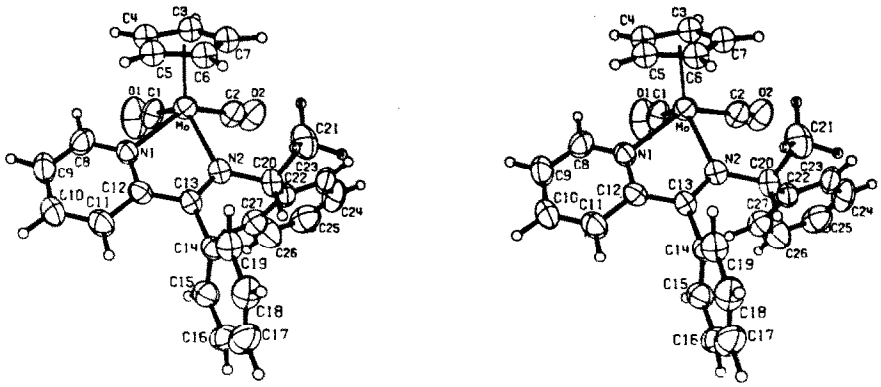

Fig. 1. Stereo pair of the cation of **2**.

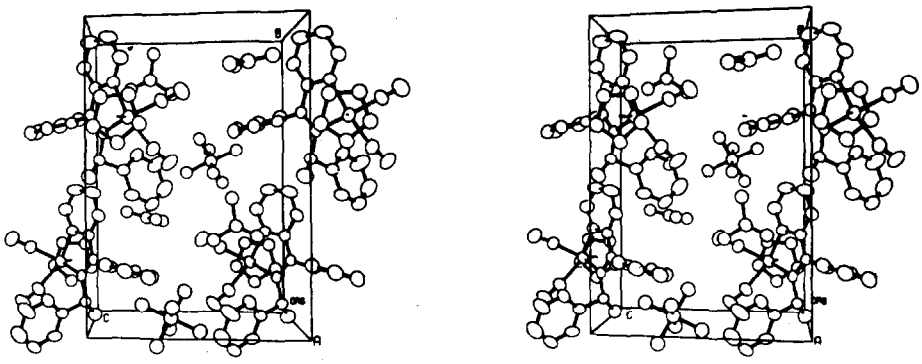

Fig. 2. Packing diagram of **2**.

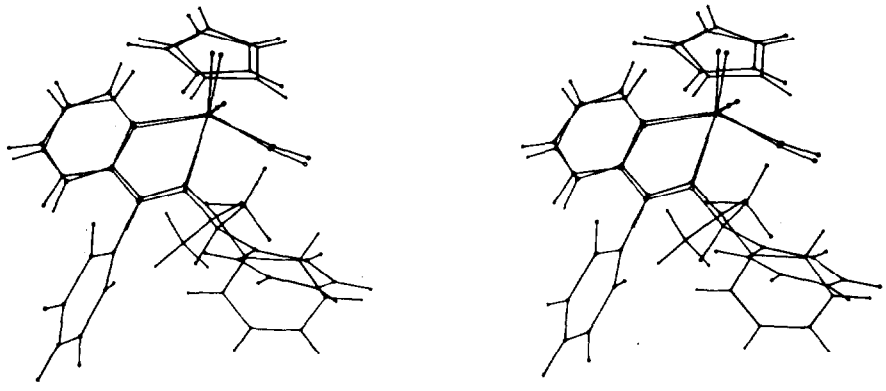

Fig. 3. Stereo plot of the cations of **1** and **2** superimposed onto one another.

TABLE 5

DETERMINATION OF THE ABSOLUTE CONFIGURATION OF **2** [16] (Radiation: Cu-K_α, λ 1.5418; −90°C)

$h\,k\,l$	$F_{obs}(+++)$	$F_{obs}(---)$	σ	$F_{obs}(+++)/F_{obs}(---)$	$F_{calc}(+++)/F_{calc}(---)$
0 1 3	50.3	55.9	0.3	0.900	0.879
0 3 2	62.3	70.4	0.3	0.885	0.897
0 3 4	95.4	81.7	0.4	1.168	1.111
0 4 5	42.6	36.1	0.3	1.180	1.097
1 1 6	63.5	59.1	0.4	1.075	1.091
1 2 2	113.1	102.3	0.3	1.106	1.092
1 5 0	47.1	44.1	0.3	1.068	1.081
2 1 0	79.9	68.3	0.3	1.170	1.158
2 1 2	170.8	162.2	0.3	1.053	1.056
2 2 0	59.3	55.2	0.3	1.074	1.073
2 3 0	98.0	87.9	0.3	1.115	1.075
2 4 0	60.0	55.4	0.4	1.083	1.077
2 4 2	70.2	76.8	0.4	0.914	0.917
2 8 6	55.5	54.5	0.4	1.018	1.083
3 2 1	51.7	63.4	0.4	0.815	0.861
4 3 1	61.2	48.8	0.4	1.254	1.259
4 6 1	57.4	59.5	0.4	0.965	0.923
5 1 3	57.3	63.3	0.4	0.905	0.923

TABLE 6

EQUATIONS OF LEAST SQUARES PLANES AND DEVIATIONS OF SELECTED ATOMS FROM THOSE PLANES (in Å) FOR **2**

A plane defined by C(3), C(4), C(5), C(6), C(7)

$-0.9765\,x + 0.0475\,y - 0.2103\,z + 10.519 = 0$

Mo	1.992(1)		

B plane defined by N(1), C(8), C(9), C(10), C(11), C(12) (max. dev. 0.016(13) Å)

$-0.7223\,x + 0.0193\,y - 0.6913\,z + 10.928 = 0$

Mo	−0.218(1)	C(14)	0.038(9)
N(2)	0.042(8)	C(20)	0.179(12)
C(13)	0.039(9)		

C plane defined by C(14), C(15), C(16), C(17), C(18), C(19) (max. dev. 0.045(15) Å)

$-0.0645\,x - 0.9640\,y - 0.2579\,z + 13.674 = 0$

C13	−0.074(9)		

D plane defined by C(22), C(23), C(24), C(25), C(26), C(27) (max dev. −0.031(17) Å)

$0.7358\,x + 0.2900\,y - 0.6120\,z - 0.215 = 0$

C(20)	−0.073(12)		

E plane defined by Mo, N(1), N(2), C(12), C(13) (max dev. 0.056(8) Å)

$-0.6657\,x + 0.0142\,y - 0.7461\,z + 11.216 = 0$

Mo	−0.044(1)	C(14)	−0.144(8)
C(8)	0.119(13)	C(15)	0.969(10)
C(9)	0.026(16)	C(19)	−1.369(11)
C(10)	−0.079(16)	C(20)	0.160(12)
C(11)	−0.105(12)	H(20)	0.052(12)

Dihedral angles: A,B 31.6°; A,C 85.9°; A,D 125.2°; A,E 36.1°; B,C 78.1°; B,D 95.9°; B,E 4.5°; C,D 99.7°; C,E 77.2°; D,E 91.7°

[4,5,20–22] was used. Thus, upon fractional crystallization, the less soluble pair of enantiomers *RR/SS* undergoes spontaneous resolution. The crystal used for the X-ray structure determination, having *RR*-configuration was dissolved in acetone; the optical rotation of the solution was positive at 546, but negative at 436 and 365 nm.

Discussion

The atoms used as input to BMFIT [14] in the least squares fit for preparation of the superimposed drawing of cations **1** and **2** in Fig. 3 were Mo, O(1), O(2), N(1), N(2), C(1), C(2), C(8)–C(13). The Mo–C(1)–O(1) fragments in **1** and **2** agree perfectly in the superposition, but, all the other parts of the cations **1** and **2** show small but distinct differences, caused by the introduction of Ph in place of H and the change in configuration at the optically active carbon atom C(20) from (*S*) to (*R*).

In compound **2** the imino carbon C(13) bears a phenyl substituent C(14)–C(19), which, as usual, is almost perpendicular to the Mo–N(1)–C(12)–C(13)–N(2) plane, as is apparent from the torsional angle C(12)–C(13)–C(14)–C(15) 73.4° and the dihedral angle C,E of 77.2°. As can be seen from the double stereodiagram of Fig. 3 the large phenyl substituent at the imino carbon C(13), in cation **2**, causes two changes with respect to cation **1**, namely (1) the pyridine ring is pushed away from

phenyl C(14)–C(19) so that its 3-hydrogen moves away from the phenyl-π-cloud, and (2), more importantly the conformation of the CH(Me)(Ph) substituent at N(2) is changed.

It has been shown previously that a large substituent, such as a C_6H_5, on the carbon atom of an imino group adjacent to an 1-phenylethyl group located at the nitrogen atom of a planar chelate ring, forces the H substituent of CH(Me)(Ph) into the chelate plane, eclipsing the C_{imino}–C_{ipso} bond [6–8]. In such a conformation the Me and Ph groups of CH(Me)(Ph) avoid severe steric hindrance with the Ph substituent at the imino carbon atom. Cation **2** confirms strictly with these previous results of conformational analyses. For compounds carrying a H substituent at the imino carbon atom the conformational preferences of a C*H(Me)(Ph) substituent at the adjacent N atom are less clear, conformations with either C*–H or C*–Me eclipsing C_{imino}–H being favorable [6,10]. For cation **1**, a torsional angle C_{imino}–N–C*–Me of $-36.1°$ was found, with Me above the MoNCCN chelate plane oriented towards the Cp ring [4]. Thus, in contrast to the conformation of **1**, the methyl group C(21) points directly towards the Cp ring in cation **2** because C*–H lies in the chelate plane (Fig. 1). This CH(Me)(Ph) conformation in **2** causes severe steric interactions between methyl group C(21) and Cp which are not present in **1**.

The C(6)–H(6) bond on Cp lies almost exactly over N(2) in compound **2** and in compound **1**. However, compared to **1**, Cp in **2** is tilted away from methyl C(21) as can be seen from the double stereo plot in Fig. 3 and the increased N(2)–Mo–Cent angle of 122.5° (vs. 116.7° in **1**) and the decreased N(1)–Mo–Cent angle of 111.2° (vs. 116.2° in **1**). This tilting of the Cp must be attributed to the repulsion between Cp and methyl C(21). At the same time H(21B) and H(21C) try to become staggered as for the best they can in order to avoid too close contacts with the C(6)–H(6) and C(7)–H(7) bonds on Cp.

The angles Mo–C(1)–O(1) and Mo–C(2)–O(2) in **2**, 178.2 and 168.3°, differ by approximately 10°. The origin of the bending in carbonyl C(2)–O(2) lies in the fact that the phenyl group C(22)–C(27) of the C*H(Me)(Ph) substituent faces C(2)–O(2). The exposure of the face of the phenyl ring C(22)–C(27) to carbonyl C(2)–O(2) implies that the two π-clouds interact so as to rehybridize C(2) towards sp^2. Such sterically bent carbonyls are known for a wide variety of systems [23–25]. In **1**, Mo–C(1)–O(1) with 177° is almost linear, whereas Mo–C(2)–O(2) with 173° is slightly bent [4], because the phenyl of the CH(Me)(Ph) substituent in this complex is also oriented towards C(2)–O(2). Due to a clockwise rotation around C*–N, however, the interaction phenyl/C(2)–O(2) is much less effective in **1** (angle at C(2) 173°) than in **2** (angle at C(2) 168.3°).

The two Mo–C(O) distances in **1** are similar (1.984 and 1.988 Å) but this is not the case for **2** in which the distances are 1.918 and 2.007 Å, Mo–C(2) (the bent CO) being longer, and this also points to a change of hybridization of C(2). Such a lengthening upon rehybridization is common in M–NO systems [26]. There is also a slight shortening of C(2)–O(2) compared with C(1)–O(1) in **2** (Table 3), but its significance is somewhat tenuous.

The greater interaction of phenyl C(22)–C(27) with C(2)–O(2) in **2** than in **1**, and especially the steric pressure of methyl C(21) on Cp, affects CH(Me)(Ph), N(2), and the whole chelate system N(2)–C(13)–C(12)–N(1) by making Mo–N(2) longer in **2** (2.228(8) Å) than in **1** (2.182(10) Å) and N(1)–Mo shorter in **2** (2.180(8) Å) than in **1** (2.258(11) Å).

In spite of the distinct differences between **1** and **2**, the C–H bonds of the Cp rings are still in a similar relation to the basal $Mo(CO)_2NN'$ fragment. In particular, in both cases C(3)–H(3) is staggered between the two carbonyls, as can readily be seen for the molecule at the upper right hand corner of the packing diagram (Fig. 2). In such an orientation carbon atoms C(5) and C(6) are as nearly eclipsed as possible with respect to N(1) (N(1)–Mo–Cent–C(5) 7.3° in **1** and 8.7° in **2**) and N(2) (N(2)–Mo–Cent–C(6) −6.1° in **1** and −2.2° in **2**), a conformation which is in accord with all known cases of square based pyramidal species in which the base is of the type $M(CO)_2NN'$ or $M(CO)_2NS$ [11]. The small differences in torsional angles N(1)–Mo–Cent–C(5) and N(2)–Mo–Cent–C(6) observed for **1** and **2** are caused by the steric requirements of methyl C(21), which is differently oriented in **1** and **2** as a result of the inversion of chirality at C(20).

The pyridine imine ligands present in compounds **1** and **2** have been used in homogeneous rhodium catalysts in the enantioselective hydrosilylation of acetophenone to give 1-phenylethanol in high optical yields [27]. In this approach to enantioselectivity, the direct interaction of a 1-phenylethyl group with the catalytically active coordination sites in a homogeneous catalyst is the crucial feature [28], whereas with optically active phosphines as chirality transmitters it is usually the $P(Ph)_2$ groups which are necessary to convey the chiral information from the optically active ligand backbone to the metal coordination positions [29]. In order to describe unequivocally the position and arrangement of the optically active C*H(Me)(Ph) substituent with respect to other coordination sites, the following parameters exemplified for **1** and **2** in Table 7, are specified: (a) the bond lengths and bond angles, I–IV, define the geometry of the M–N–C* unit; (b) the torsional angle, V, defines the deviation of C* from the chelate plane; (c) the torsional angles, VI–VIII, define the conformation of C*H(Me)(Ph); (d) the torsional angle IX defines the orientation of the phenyl plane. All these parameters are relevant for the interaction of the chiral CH(Me)(Ph) and similar substituents with the adjacent metal coordination sites.

A "face-to-edge" orientation of two phenyls (or a phenyl and a Cp) is known to be a favorable configuration [29,30]. It is evident from the packing diagram in Fig. 2 that in the lattice such intermolecular "face-to-edge" arrangements in **2** are present

TABLE 7

PARAMETERS I–IX, DEFINING THE ORIENTATION OF C*H(Me)(Ph) WITH RESPECT TO OTHER COORDINATION SITES FOR **1** AND **2**

		2	**1**
I	Mo–N(2)	2.228(8) Å	2.182(10) Å
II	N(2)–C(20)	1.477(15) Å	1.486(15) Å
III	N(1)–Mo–N(2)	73.2(3)°	74.0(4)°
IV	Mo–N(2)–C(20)	126.0(7)°	123.4(8)°
V	N(1)–Mo–N(2)–C(20)	174.7°	−172.7°
VI	Mo–N(2)–C(20)–C(22)	−71.4°	−97.7°
VII	Mo–N(2)–C(20)–C(21)	55.6°	135.3°
VIII	Mo–N(2)–C(20)–H(20) [a]	172.1°	17.2°
IX	N(2)–C(20)–C(22)–C(27)	−42.1°	−62.1°

[a] Calculated on the basis of tetrahedral geometry at C(20) with idealized position for H(20).

between the phenyl C(22)–C(27) ring of one molecule and the pyridine ring as well as the phenyl group C(14)–C(19) of a neighbouring molecule. The PF_6^- anions are not engaged in intermolecular interactions, as shown by the high thermal parameters, and the acetone molecules are imbedded in large channels along *b* from which they can obviously escape, as shown by the decay of intensity caused by lattice loss of acetone (i.e., the 70% "occupancy" found upon refinement). During the low temperature (−90°C) alignment of the crystal [16] it was noted that there was a marked volume contraction of about 4.6% with the largest change in cell constants along a (10.361(4) Å vs. 10.001(5) Å). The packing diagram shows that the acetone molecules lie in large holes such that along a, the acetone molecule being far from any other molecular fragment.

Acknowledgements

H.B. and D.K.R. thank the Deutsche Forschungsgemeinschaft, the Fonds der Chemischen Industrie, and the BASF AG for support of this work. I.B. and W.H.R. thank the Robert A. Welch Foundation for research support, NATO for a Fellowship (W.H.R.), I.B. thanks the Alexander von Humboldt-Stiftung for a U.S. Senior Scientist Award and D.K.R. for a fellowship. We also thank Dr. Charles F. Campana of Nicolet XRD Corporation, Cupertino (CA) for the low temperature (−90°C) determination of the I_0 values for the Bijvoet pairs (Cu-K_α).

References

1 Part LXXX: H. Brunner, H. Weber, I. Bernal, and G.M. Reisner, Organometallics, 3 (1984) 163.
2 H. Brunner and W.A. Herrmann, Chem. Ber., 105 (1972) 3600.
3 H. Brunner and W.A. Herrmann, Chem. Ber., 106 (1973) 632.
4 I. Bernal, S.J. LaPlaca, J. Korp, H. Brunner, and W.A. Herrmann, Inorg. Chem., 17 (1978) 382.
5 H. Brunner, Adv. Organomet. Chem., 18 (1980) 151.
6 H. Brunner, G. Agrifoglio, I. Bernal, and M.W. Creswick, Angew. Chem., Int. Ed. Engl., 19 (1980) 641.
7 I. Bernal, M. Creswick, H. Brunner, and G. Agrifoglio, J. Organomet. Chem., 198 (1980) C4.
8 H. Brunner, G. Agrifoglio, R. Benn, and A. Rufińska, J. Organomet. Chem., 217 (1981) 365.
9 H. Brunner, and D.K. Rastogi, Inorg. Chem., 19 (1980) 891.
10 H. Brunner, and D.K. Rastogi, Bull. Soc. Chim. Belg., 89 (1980) 883.
11 M.W. Creswick, and I. Bernal, in preparation; see M.W. Creswick, Ph.D. Thesis, University of Houston, 1981.
12 G.M. Sheldrick, SHELX-76, A Program for Crystal Structure Determination; Cambridge University, Cambridge, 1976.
13 C.K. Johnson, ORTEP 2, A Fortran-Ellipsoid Plot Program for Crystal Structure Illustration, ORNL-5138, Oak Ridge, Tenn., 1972.
14 BMFIT, L.-K. Liu, University of Texas, Austin, 1977, based upon S.C. Nyburg, Acta Crystallogr., B30 (1974) 251.
15 J.M. Bijvoet, A.F. Peerdeman and A.J. van Bommel, Nature (London), 168 (1951) 271.
16 For the Bijvoet test Cu-K_α radiation was used because with Mo-K_α radiation only 4 reflections showed small but barely significant differences.
17 E. Ruch, and A. Schönhofer, Theor. Chim. Acta, 10 (1968) 91.
18 E. Ruch, Theor. Chim. Acta, 11 (1968) 183.
19 E. Ruch, Angew. Chem., Int. Ed. Engl., 16 (1977) 65.
20 C. Lecomte, Y. Dusausoy, J. Protas, J. Tirouflet, and A. Dormond, J. Organomet. Chem., 73 (1974) 67.
21 K. Stanley, and M.C. Baird, J. Am. Chem. Soc., 97 (1975) 6598.

22 R.S. Cahn, C.K. Ingold, and V. Prelog, Angew. Chem. Int. Ed. Engl., 5 (1966) 385.
23 G.M. Reisner, I. Bernal, and G.R. Dobson, J. Organomet. Chem., 157 (1978) 23.
24 G.M. Reisner, I. Bernal, and G.R. Dobson, Inorg. Chim. Acta, 50 (1981) 227.
25 G.M. Reisner, I. Bernal, and G.R. Dobson, Inorg. Chem., in press.
26 J.H. Enemark, and R.D. Feltham, Coord. Chem. Rev., 13 (1974) 339.
27 H. Brunner, and G. Riepl, Angew. Chem. Suppl., 21 (1982) 769.
28 H. Brunner, in A. Müller, and E. Diemann, Transition Metal Chemistry, Current Problems of General, Biological and Catalytical Relevance, Verlag Chemie, Weinheim, Deerfield Beach, Basel, 1982, p. 265.
29 H. Brunner, A.F.M.M. Rahman and I. Bernal, Inorg. Chim. Acta, 83 (1984) L93.
30 W.S. Knowles, B.D. Vineyard, M.J. Sabacky, and B.R. Stults, Fundamental Research in Homogeneous Catalysis, 3 (1979) 537.